THE AMERICAN MINERALOGIST, VOL. 55, JULY-AUGUST, 1970

THE CRYSTAL CHEMISTRY OF CHABAZITES

ELIO PASSAGLIA, *Istituto di Mineralogia dell' Università di Modena, Italy.*

ABSTRACT

After an examination of the chemical analyses of chabazites reported in literature, 28 samples have been selected for detailed study. The chemical analyses, unit-cell dimensions, refractive indices and densities of these samples are given. The X-ray diffraction powder patterns, DTA curves and a description of the behavior on heating of three samples are reported. The correlations between chemical and physical properties are determined. Equations for estimating the Si/(Si+Al+Fe) ratio and the sum of exchangeable cations from the measured values of a and c are calculated, as well as the ratio between the sum of monovalent cations and the sum of all exchangeable cations from the measured value of ω. The results of the chemical analyses exclude the presence of a compositional gap between Ca and Na end-members.

INTRODUCTION

Chabazite is a rhombohedral zeolite; the chemical content of its unit cell varies, according to Coombs *et al.* (1959), from (Ca, Na_2, K_2)$_5Al_{10}Si_{26}O_{72}\cdot 36H_2O$ to (Ca, Na_2, K_2)$_{6.75}Al_{13.5}Si_{22.5}O_{72}\cdot 36H_2O$. Wyart (1933) determined its cell constants; Dent and Smith (1958) and Nowacki *et al.* (1958a) resolved its structure. Recently several authors [Smith (1962); Smith *et al.* (1963); and Smith *et al.* (1964)] refined the structure offering persuasive evidence for the triclinic symmetry of this mineral, predicted by Becke (1880). Barrer and Sammon (1955) studied the possible ion exchanges, and Barrer (1958) pointed out that the cation substitutions in the lattice cause small changes of the cell constants. Studies on the thermal behavior of this mineral were performed by several authors [Koizumi (1953); Majer (1953); Mason and Greenberg (1954); and Pécsi-Donáth (1965)].

The object of this work is to establish the actual chemical variability of chabazite and the relations between its chemical composition and physical properties (cell constants, X-ray diffraction powder pattern, density, refractive indices, thermal behavior).

EVIDENCE FROM LITERATURE DATA

In order to get a general idea of the chemical variations shown by this zeolite and thereby define the scope of the present study, all the chemical analyses of chabazites present in the literature were first examined. The chemical formula of each analysis was calculated on the basis of 24 Oxygens ($\frac{1}{3}$ of unit cell) by means of a computer. As the chemical variations chiefly concern the content of Ca, Na, and K, the atomic coefficients of these elements are recalculated so to have their sum equal to 100 and plotted in a triangular diagram with Ca, Na, K, respectively as its ver-

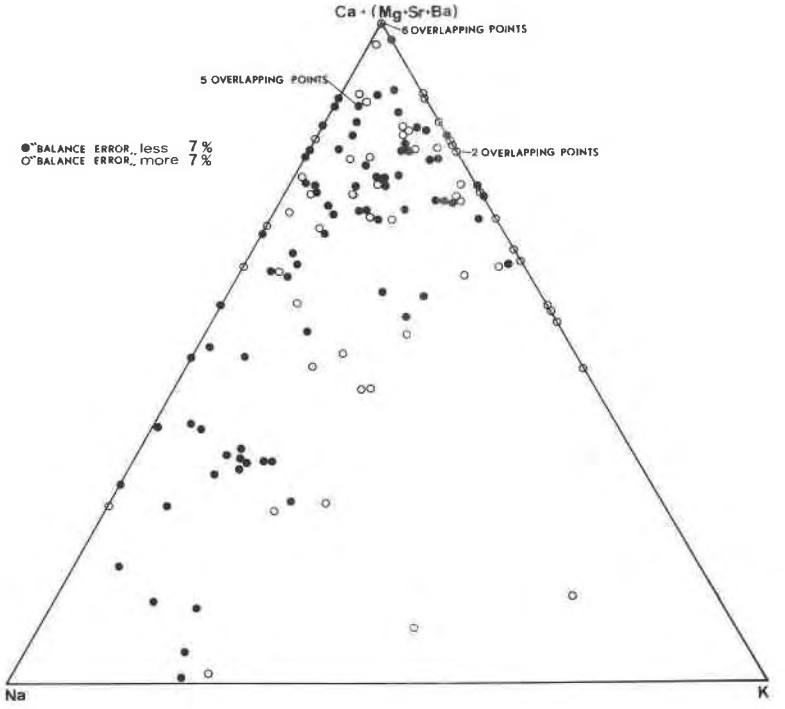

FIG. 1. Distribution of exchangeable cations in chabazites, in moles, from literature reports. Solid circles: analyses with a balance error of less than $7\mp$ percent; hollow circles: analyses with a balance error of more of $7\pm$ percent.

Sources of chemical analyses (the number in square brackets preceding the author's name indicates the quantity of chemical analyses taken from that literature source): [1] Barrer and Sammon (1955); [1] Breck et al. (1956); [1] Caglioti (1927); [1] Capola (1948); [1] Černý and Povondra (1965); [98] Doelter (1921); [1] Dunham (1933); [1] Gude and Sheppard (1966); [2] Herbert Smith (1916); [1] Hewett et al. (1928); [1] Hodge-Smith (1929); [1] Irrera (1949); [1] Kappen and Fischer (1928); [1] Kato (1959); [1] Koizumi (1953); [1] Kostov (1962); [1] Majer (1953); [1] Mason (1955); [1] Morgante (1945); [1] Niggli et al. (1940); [3] Pécsi-Donáth (1965); [1] Rabinowitch and Wood (1936); [2] Reichert and Erdelyi (1935); [1] Shkabara (1941); [10] Stoklossa (1918); [1] Tiselius and Brohult (1934); [1] Tomkeieff (1934); [3] Walker and Parsons (1922); [1] Weibel (1963).

tices (Fig. 1). The atomic coefficients of Ba, Sr and Mg are added to Ca.

In order to recognize "reliable analyses," a "balance error" of every analysis between the atomic coefficient of the exchangeable cations and the atomic coefficient of $Al(+Fe^{3+})$ was calculated. This balance error is calculated by the following formula:

$$E = \frac{Al(+Fe^{3+}) - Al_{theor.}}{Al_{theor.}} \times 100$$

where $Al_{theor.} = Na+K+2(Ca+Mg+Sr+Ba)$, and $Al(+Fe^{3+})$ is the

atomic coefficient of Al plus the coefficient of Fe^{3+} given by the analysis. Obviously, a positive error shows an excess of trivalent cations, while a negative error an excess of exchangeable cations. The meaning of this error is easily understood if it is borne in mind that in chabazite, as in all the framework-silicates, the presence of one monovalent cation corresponds to the substitution of one Si with one Al, while the presence of one bivalent cation corresponds to the substitutions of two Si with two Al. In the analyses where Fe was present it was considered completely as Fe_2O_3, so that in the calculation of the balance error, its atomic coefficient was added to that of Al.

In plotting the analyses in the diagram those with a balance error of less than ± 7 percent, are marked with a solid circle, while all the others are marked with an empty circle.

In the diagram of Figure 1, a strong concentration of samples near the vertex Ca (+Mg+Sr+Ba) occurs, as well as a good number of samples near the vertex Na, while the area near the vertex K is almost deserted (only one sample). Moreover, a certain number of samples fall in the area between those rich in Ca and those rich in Na; so that it seems that a gradual transition occurs between the two extreme terms. Then there are some samples which are slightly displaced towards the vertex K, though they remain in the middle part of the diagram. For present purposes this distribution was taken into account in the selection of samples to be examined and the following were chosen: some of those falling near the vertex Ca; two falling near the vertex Na; almost all those falling in the average area between the two vertices above mentioned; and those falling in the area displaced towards the vertex K. Furthermore, other samples of chabazite from hitherto unexplored localities were analyzed. Samples described in the literature were considered only if: 1) chemical analyses were reliable; 2) unit cell data and/or X-ray diffraction powder data were available. Chemical analyses were considered reliable if the balance errors were less than ± 10 percent. 5 samples with their chemical analyses were kindly furnished by P. Černý.

Samples Studied

In this work a total of 28 samples is taken into account, most of them studied by the author of this paper. These samples are listed in Table 1. Only for a few samples data from other sources were utilized, as follows: the chemical analyses of samples 22–25 from Černý (analyst P. Povondra), that of "No. 21" from Mavrudčiev *et al.* (1965); chemical analysis of "No. 26" from Niggli *et al.* (1940), unit cell dimensions from Nowacki *et al.*, (1958b); chemical analysis and X-ray diffraction powder data of samples Nos. 27 and 28 respectively from Weibel (1963) and from Gude and Sheppard (1966).

Experimental

The chemical composition, unit-cell dimensions, density and refractive indices of the samples were determined. Three samples, (Nos. 1, 4, and 13), were studied with DTA and

TABLE 1. LIST OF SAMPLES

No.	Locality of occurrence.	Habit and paragenesis.	Reference for preceeding description, if any.	Donor (if not collected by the author of owned by Modena University).
1	Biggest "Faraglione" facing Acitrezza (Sicily, Italy).	Spherical aggregates of Hexagonal plates in basalt with phillipsite.		
2	Cliffs facing the Rupe of Aci Castello (Sicily, Italy).	Little white transparent grains easily cleaved in basalt with natrolite.	Di Franco (1942)	
3	Palagonia (Sicily, Italy).	White transparent prismatic aggregates of hexagonal plates in basalt.	Di Franco (1942) Capola (1948)	M. Riuscetti (Catania)
4	Casal Brunori (Rome, Italy). Quarry near km 4.5 on Via Pontina.	Milky white crystals twinned with spherical shape, diameter 1–5 mm, in leucitite with phillipsite	Zambonini (1902)	
5	Vallerano (Rome, Italy). Quarry at the intersection of Via Lauretina with "Raccordo" Anulare"	As No. 4	Zambonini (1902)	
6	Acquacetosa (Rome, Italy). Abandoned quarry near km 8.5 on Via Laurentina.	As No. 4	Zambonini (1902)	
7	Osa (Rome, Italy). Quarry near km 18 on Via Prenestina.	As No. 4		
8	Striegau (Silesia, Poland)	Rhombohedral brick-red crystals on quartz crystals.	Rimatori (1900)	
9	Vaalvo—(Färöer, Denmark)	White transparent rhomboedral crystals twinned in spherical shape with phillipsite		M. Franzini (Pisa)
10	Nova Scotia (Canada)	Rhombohedral salmon-red crystals.	Walker and Parsons (1922)	
11	Valle Rossa (Cene, Bergamo, Italy).	Rhombohedral white transparent or yellow-colored crystals in porphyrite.		G. Scaini (Milano)
12	Miage (Monte Blanc, Italy)	Rhombohedral yellow or yellow-brown colored crystals in biotite-gneiss.	Scaini and Giorgetta (1967)	G. Scaini (Milano)
13	Col del Lares (Val di Fassa, Italy).	Rhombohedral white transparent crystals in Triassic porphyrite.		
14	Piatto (Biella, Italy). Near km 13.3 of Zegna-Bielmonte road.	Little transparent rhombohedra in amphibole gabbro.	De Michele and Scaini (1968)	V. De Michele (Milano)
15	Albero Bassi (Vicenza, Italy). In pebbles of a left branch of the Timonchio stream.	Spherical grains brick-red colored by Fe-oxides in Triassic porphyrite with heulandite.	Passaglia (1969)	
16	Richmond (Victoria-Australia)	White transparent crystals twinned with spherical shapes (up to 1 cm) in basalt.		R. J. W. McLaughlin (Melbourne)

TABLE 1 (*contined*)

No.	Locality of occurrence.	Habit and paragenesis.	Reference for preceeding description, if any.	Donor (if not collected by the author of owned by Modena University).
17	Kyogle (N.S.W., Australia)	White transparent crystals	Hodge-Smith (1929)	R. J. W. McLaughlin (Melbourne)
18	Collingwood (Victoria, Australia)	White transparent crystals twinned with big spherical shapes (1 cm in diameter) in basalt.		R. J. W. McLaughlin (Melbourne)
19	2 Miles of N.E. of Gads Hill (Middlesex, N.W. Tasmania)	Dark-white crystals twinned with big spherical shapes.		Tasmanian Museum of Hobart.
20	Jones Falls (Maryland U.S.A.)	Rhombohedral dark-red crystals remarkably large on sandstone.	Morse et al. (1884)	U. S. National Museum No. C 3514
21	Madžarovo (Bulgaria).	White transparent crystals twinned with spherical shapes.	Mavrudčiev et al. (1965).	P. Černý
22	Dunabogdány (Hungary).	Pale-pink crystals.	Pécsi-Donáth (1965).	P. Černý
23	Sobotín Štětínov (N. Moravia, Czechoslovakia).	Powdered sample.		P. Černý
24	Kozákov near Turnov (N. Bohemia, Czechoslovakia).	Little transparent crystals in subspherical shapes.		P. Černý
25	Kozákov near Turnov (N. Bohemia, Czechoslovakia).	Big transparent crystals in subspherical shapes.		P. Černý
26	Schattig Wichel (Switzerland).	Sample not examined by the author.	Niggli et al. (1940); Nowacki et al. (1958b).	
27	Chrüzlistock (Tavetsch, Switzerland).	Sample not examined by the author.	Weibel (1963).	
28	Fossil Canyon (S. Bernardino County, California U.S.A.)	Sample not examined by the author.	Gude and Sheppard (1966).	

with X-ray diffraction powder patterns on samples previously heated at different temperatures.

In the chemical analysis, the classic analytic procedures were used for the determination of H_2O and SiO_2; Al_2O_3 was determined by the volumetric complexometric method (Charlot, 1961, p. 587). The other elements were determined by the Perkin-Elmer 303 atomic absorption spectrometer.

In the determination of unit-cell dimensions the spacings were measured on a Philips diffractometer, calibrated with the lines at 4.260, 3.343, 2.458, 2.287, 2.237, 2.128, 1.980, and 1.817 Å of quartz. The unit-cell dimensions were calculated with an IBM 1620 computer using a least squares program. The spacings were indexed following Gude and Sheppard (1966). Only spacings from 4.5 and 1.81 Å were used for this calculation.

The densities were determined using a torsion microbalance with toluene according to Berman (1939). Refractive indices were measured on the U-stage by the Emmons double variation method. The DTA curves on samples 1, 4 and 13 were obtained with a thermal

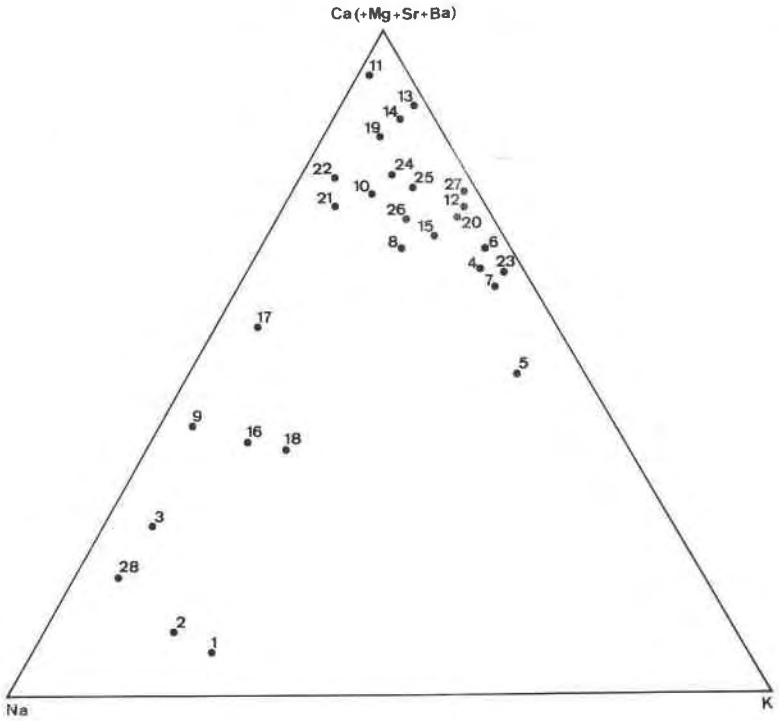

FIG. 2. Distribution of exchangeable cations, in moles, in studied chabazites.

analyser manufactured by B.D.L. (Bureau de Laison, Paris). X-ray diffraction powder photographs at low temperatures of three samples previously heated at different temperatures, were taken with a Guinier-De Wolff camera.

RESULTS AND THEIR VARIABILITY

The 28 analyses used to study the composition of chabazites are given with their atomic ratios and balance error in Table 2. The differences of content in exchangeable cations are illustrated in Figure 2. In this figure, the analyses are plotted in terms of molecular percentage of the components Ca(+Mg+Sr+Ba), Na and K. It is observed that samples almost corresponding to Ca-end members and to Na-end members exist; the points corresponding to several samples almost completely fill the gap between the Ca and Na vertices; there are no samples with K prevailing over the other cations, but samples exist in which, although Ca prevails, the K content is also high and in these cases the Sr content is remarkable too.

The compositional relationship and differences of the content of SiO_2

TABLE 2. CHEMICAL ANALYSES AND ATOMIC RATIOS OF CHABAZITES

	1	2	3	4	5	6	7	8	9	10	11	12	13	14
SiO_2	42.45	44.97	49.33	38.21	38.85	38.29	37.88	47.94	45.83	50.74	42.40	48.76	46.40	48.05
Al_2O_3	22.06	20.32	18.73	22.66	22.41	22.02	22.54	17.64	18.98	16.56	19.23	17.71	19.30	18.41
Fe_2O_3	0.11	0.17	0.06	0.10	0.10	0.15	0.14	1.29	0.07	0.14	0.08	0.13	0.06	0.06
MgO	0.24	0.07	0.02	0.04	0.06	0.07	0.10	0.40	0.02	0.09	0.02	0.09	0.06	0.23
CaO	1.01	1.78	4.00	6.57	5.25	6.91	6.62	7.05	6.02	7.52	7.35	7.10	10.04	8.40
SrO	0.47	0.30	0.12	5.27	3.78	4.40	5.34	0.44	0.10	0.49	5.69	1.46	0.32	1.34
BaO	<0.01	0.04	<0.01	0.90	0.80	1.28	0.49	0.19	0.04	0.06	0.03	0.04	0.02	0.04
Na_2O	9.20	8.66	5.99	0.48	0.78	0.25	0.42	0.92	4.68	0.81	0.31	0.17	0.10	0.27
K_2O	4.70	3.07	0.86	3.89	5.76	3.62	4.55	1.85	0.56	0.94	0.15	2.18	0.92	0.80
H_2O^+	16.39	16.02	18.95	17.02	17.01	20.38	18.08	19.33	22.14	20.59	19.10	19.27	20.93	18.98
H_2O^-	3.34	4.15	2.37	4.42	4.37	2.00	3.86	2.36	2.15	1.86	4.72	2.73	1.87	3.42
Total	99.97	99.55	100.43	99.56	99.17	99.37	100.02	99.41	100.59	99.80	99.08	99.64	100.02	100.00
Si	7.40	7.79	8.30	7.05	7.17	7.14	7.02	8.28	8.04	8.60	7.80	8.41	8.03	8.26
Al	4.53	4.15	3.72	4.93	4.87	4.84	4.92	3.59	3.93	3.38	4.17	3.60	3.94	3.73
Fe	0.01	0.02	0.01	0.01	0.01	0.02	0.02	0.17	0.01	0.02	0.01	0.02	0.01	0.01
Mg	0.06	0.02	0.01	0.01	0.02	0.02	0.03	0.10	0.01	0.02	0.01	0.02	0.02	0.06
Ca	0.19	0.33	0.72	1.30	1.04	1.38	1.31	1.30	1.13	1.39	1.45	1.31	1.86	1.55
Sr	0.05	0.03	0.01	0.56	0.40	0.48	0.57	0.04	0.01	0.05	0.61	0.15	0.03	0.13
Ba	<0.01	<0.01	<0.01	0.07	0.06	0.09	0.04	0.01	<0.01	<0.01	<0.01	<0.01	<0.01	<0.01
Na	3.11	2.91	1.96	0.17	0.28	0.09	0.15	0.31	1.59	0.27	0.11	0.06	0.03	0.09
K	1.05	0.68	0.18	0.92	1.36	0.86	1.08	0.41	0.13	0.21	0.04	0.48	0.20	0.18
O	24.00	24.00	24.00	24.00	24.00	24.00	24.00	24.00	24.00	24.00	24.00	24.00	24.00	24.00
H_2O	11.47	11.65	11.97	13.20	13.16	13.91	13.55	12.49	14.22	12.95	14.61	12.66	13.16	12.84
E	−4.30	−4.10	+2.99	−0.45	+4.71	−0.59	−3.63	+2.09	−2.05	−0.72	−2.14	+3.23	−2.78	−0.31

and Al_2O_3 are illustrated in a triangular diagram with $Si_{12}O_{24}$, (Ca, Mg, Sr, Ba)$_3Al_6Si_6O_{24}$ and (Na, K)$_6Al_6Si_6O_{24}$ at its vertices (Fig. 3). Most of the samples fall in the area limited by 7.80 and 9.00 of Si in terms of atomic coefficients. Five samples (Nos. 1, 4, 5, 6, 7) fall under 7.80 of Si and only one (No. 28) above 9.00 of Si.

The content of H_2O is also variable. It ranges from a minimum of 10.10 molecules (No. 28) to a maximum of 15.25 (No. 15). It depends both on the Si/Al ratio and on the exchangeable cation prevailing in the mineral. In this context Foster (1965) noted that, in fibrous zeolites, the water content is lower in Na rich members than in Ca rich members. A similar relationship in ion-exchanged chabazite was also noted by Barrer and Sammon (1955).

In Table 3 the unit-cell dimensions are listed. The use of hexagonal lattice constants was preferred although the mineral is rhombohedral. The lattice constants of No. 26 were not utilized because they were measured by a different method (rotating crystal) from that used for all other samples. The variability of the lattice constants *a* and *c* is illustrated in Figure 4. The points occur along a line almost parallel to *c*, with a slight inclination.

TABLE 2 (*continued*)

15	16	17	18	19	20	21	22	23	24	25	26	27	28
49.34	45.52	48.02	46.50	47.26	53.42	47.93	49.36	50.02	50.00	50.04	49.00	48.10	59.68
15.35	20.04	18.61	18.64	18.05	16.32	18.96	17.51	17.28	17.01	16.81	18.17	17.80	13.11
0.97	0.04	<0.01	0.04	<0.01	0.61	0.02	—	—	—	—	0.38	—	0.13
0.56	0.04	0.02	0.02	0.04	1.21	0.10	—	0.42	—	0.06	—	—	0.79
5.40	5.55	6.80	5.35	9.08	4.77	9.05	8.06	6.41	6.25	8.15	9.04	5.30	1.13
0.60	0.68	0.45	0.46	0.08	0.33	n.d.	0.40	0.49	1.99	0.40	n.d.	4.00	n.d.
0.40	0.34	0.17	<0.01	<0.01	1.32	n.d.	1.16	0.77	2.06	0.56	—	0.70	n.d.
0.47	4.32	2.76	3.76	0.50	0.24	1.34	1.06	0.17	0.56	0.51	0.78	0.10	5.30
1.76	1.71	0.59	2.34	0.68	1.98	0.71	0.44	3.36	1.04	1.46	1.79	1.90	0.62
21.97	16.81	18.27	18.47	19.78	17.74	15.88	15.77	15.05	14.75	15.88	16.19	}	10.25
3.65	4.91	4.15	3.99	4.08	1.96	6.09	6.41	6.57	6.65	5.96	4.67	21.90 }	8.76
100.47	99.96	99.84	99.57	99.55	99.90	100.08	100.17	100.54	100.31	99.83	100.02	99.80	99.83
8.80	7.90	8.25	8.14	8.27	8.81	8.16	8.44	8.52	8.58	8.55	8.27	8.41	9.51
3.23	4.10	3.77	3.85	3.72	3.17	3.80	3.53	3.47	3.44	3.39	3.62	3.67	2.46
<0.01	0.01	<0.01	0.01	<0.01	0.08	<0.01	—	—	—	—	0.05	—	0.02
0.15	0.01	0.01	0.01	0.01	0.29	0.03	—	0.11	—	0.02	—	—	0.19
1.03	1.03	1.25	1.00	1.70	0.84	1.65	1.48	1.17	1.15	1.49	1.64	0.99	0.19
0.06	0.07	0.04	0.05	0.01	0.03	n.d.	0.04	0.05	0.20	0.04	n.d.	0.41	n.d.
0.03	0.02	0.01	<0.01	<0.01	0.09	n.d.	0.08	0.05	0.14	0.04	—	0.05	n.d.
0.16	1.45	0.92	1.28	0.17	0.08	0.44	0.35	0.06	0.19	0.17	0.26	0.03	1.64
0.40	0.38	0.13	0.52	0.15	0.42	0.15	0.10	0.73	0.23	0.32	0.39	0.42	0.13
24.00	24.00	24.00	24.00	24.00	24.00	24.00	24.00	24.00	24.00	24.00	24.00	24.00	24.00
15.25	12.57	12.85	13.11	13.92	10.84	12.47	12.66	12.28	12.24	12.44	11.75	12.77	10.10
+3.95	+0.12	+2.56	−1.48	−1.07	+8.24	−3.58	−2.92	−1.96	+1.64	−7.39	−6.32	+9.50	−2.05

No. 10: includes about 1% of Quartz, determined by X-ray diffractometer, and not considered in deriving atomic ratios.

No. 21 by Mavrudčiev *et a*. (1965)

No. 15: Fe_2O_3 is an impurity and, therefore, not considered in deriving atomic ratios.

No. 20: Fe_2O_3 is due both to the impurities and to the mineral. Being impossible to know their exact values, the whole Fe_2O_3 is considered as part of the mineral and this also explains the high "balance error."

Analyses No. 22 to No. 25 by P. Povondra sent to author by P. Černý.

No. 26 by Niggli *et a* . (1940).

No. 27 by Weibel (1963).

No. 28, by Gude and Sheppard (1966), includes 0.04 of TiO_2 and 0.02 of FeO to low to be considered in calculation of formula.

In Table 4 the measured and calculated densities, and the refractive indices are listed. The values of the refractive indices are plotted in a diagram ϵ, ω (Fig. 5). A uniform distribution of the samples about a line inclined at an angle of 45° is observed. The optically negative samples are under this line, while the four definitely positive ones (Nos. 8, 10, 15, 20) are above it. The samples rich in Na (Nos. 1, 2, 3, 28) are down in the left, those rich in Ca, the most abundant, in the middle and those rich in Sr (Nos. 4, 5, 6, 7, 11) up on the right part of the diagram.

The frequency distribution of the densities measured (calculated for samples 23, 26, 27, 28) is represented in Figure 6. The most common density is between 2.05 and 2.09. Only one sample (No. 28) shows a remark-

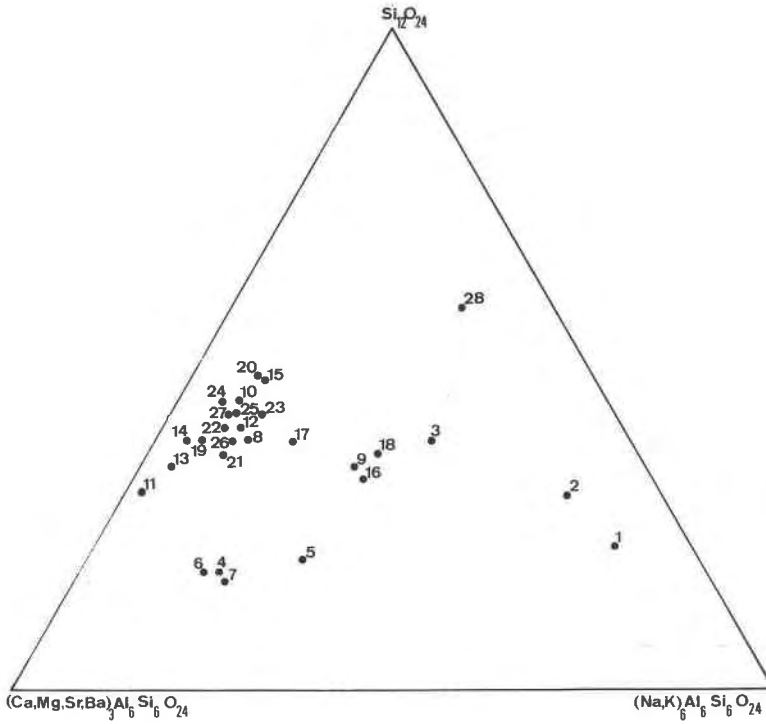

FIG. 3. Mole plot of $M_3^{2+}Al_6Si_6O_{24}$, $M_6^{+}Al_6Si_6O_{24}$, $Si_{12}O_{24}$ where $M^{2+}=Ca+Mg+Sr+Ba$ and $M^{+}=Na+K$,

ably lower value (1.97), while four samples (Nos. 4, 5, 6, 7) show very much higher values (2.18–2.20).

Relationship Between Chemical Composition and Physical Properties

Through the use of the BMD O2R stepwise multiple regression program, written by Sandi and Franchi for the IBM 7090 computer, possible correlations between the chemical and physical properties of chabazites were studied.

As already reported by Gude and Sheppard (1966), the optical parameters of zeolites depend on exchangeable cations, on the Si/Al ratio and on the degree of hydration. The ϵ and ω values of chabazites listed in Table 4 have been correlated with the following chemical variables: 1) $R=Si/(Si+Al+Fe)$; 2) $PCS=\Sigma$ [(atomic weight of an exchangeable cation)$\times$(its atomic coefficient)]; 3) $M/(M+B)$ = (sum of atomic coefficients of the monovalent exchangeable cations)/(sum of atomic co-

TABLE 3. LATTICE CONSTANTS (Å) OF THE CHABAZITES. ERROR IN BRACKETS

No.	a	c	No.	a	c
1	13.863 (3)	15.165 (3)	15	13.807 (6)	15.022 (4)
2	13.840 (4)	15.157 (4)	16	13.835 (7)	15.123 (5)
3	13.814 (5)	15.087 (3)	17	13.811 (8)	15.046 (7)
4	13.773 (3)	15.424 (4)	18	13.824 (5)	15.091 (4)
5	13.819 (18)	15.413 (17)	19	13.799 (6)	15.022 (5)
6	13.794 (4)	15.419 (8)	20	13.824 (10)	15.001 (8)
7	13.787 (7)	15.406 (7)	21	13.839 (9)	15.071 (7)
8	13.819 (9)	15.020 (6)	22	13.764 (8)	14.974 (7)
9	13.816 (7)	15.058 (6)	23	13.819 (7)	15.021 (6)
10	13.803 (7)	15.001 (6)	24	13.774 (5)	15.017 (4)
11	13.793 (5)	15.137 (5)	25	13.788 (5)	15.030 (5)
12	13.798 (5)	15.049 (4)	26	13.740 (30)	14.830 (30)
13	13.790 (5)	15.040 (4)	27	13.784 (44)	15.065 (32)
14	13.791 (6)	15.028 (5)	28	13.705 (11)	14.870 (8)

Numbers of samples are the same as Table 1.

No. 1 to No. 25: values measured by the author.

No. 26: values obtained by Nowacki *et al.* (1958b) with rotating crystal method.

No. 27: values calculated by the author from the x-ray diffraction powder data by Weibel (1963). The values reported by Weibel are: $a = 13.773$ (1); $c = 14.994$ (1).

No. 28: values calculated by the author from the x-ray diffraction powder data by Gude and Sheppard (1966). The values reported by these authors are: $a = 13.712$ (1); $c = 14.882$ (2).

efficients of all exchangeable cations); 4) number of the H_2O molecules for unit formula; 5) Fe_2O_3 weight percent. The correlations matrices obtained respectively for ϵ and ω are given in Table 5.

From the comparison of these two correlation matrices the following deduction can be made: both the indices show a major correlation with *PCS* and *R*, and a minor one with $M/(M+B)$ and H_2O. The only notable difference concerns their correlation with Fe_2O_3: it is greater for ϵ than for ω. In fact, of all the chabazites studied those optically positive are rich in Fe_2O_3. The significance of the regression equations is given by the *F* ratio value (= ratio between mean square of regression and mean square of residual). The regression equations with the greatest significance (level of probability more than 99%) for ϵ and ω are:

$$\epsilon = 1\ 46807 + 0.00036(PCS) - 0.03189[M/(M+B)] + 0.0144(Fe_2O_3)$$

$$F\text{-ratio} = 39.918$$

$$\omega = 1.47209 + 0.00036(PCS) - 0.03269[M/(M+B)]$$

$$F\text{-ratio} = 51.298$$

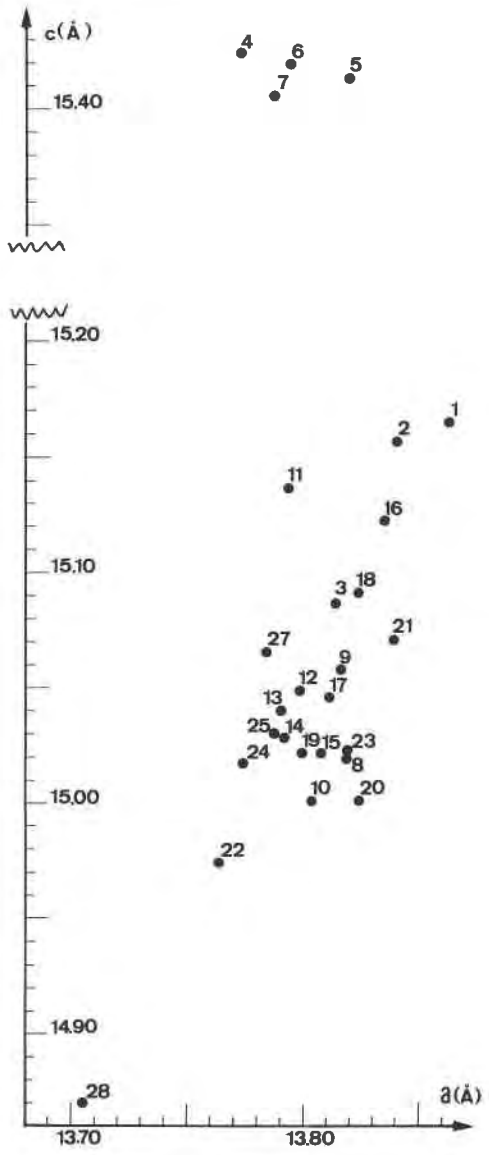

FIG. 4. Variation of lattice constants.

The unit cell dimensions (except No. 26) reported in Table 3 are correlated with the following chemical variables: 1) $R = \mathrm{Si}/(\mathrm{Si}+\mathrm{Al}+\mathrm{Fe})$; 2) $M+B =$ (sum of the atomic coefficients of all exchangeable cations);

TABLE 4. DENSITIES AND REFRACTIVE INDICES OF THE CHABAZITES

No.	ρ(meas)	ρ(calc)	ε	ω	No.	ρ(meas)	ρ(calc)	ε	ω
1	2.09± .02	2.066	1.4750	1.4773	15	2.12± .02	2.141	1.4895	1.4871
2	2.06± .01	2.051	1.4776	1.4793	16	2.09± .01	2.070	1.4879	1.4909
3	2.05± .01	2.029	1.4789	1.4805	17	2.06± .01	2.064	1.4859	1.4888
4	2.20± .01	2.170	1.5142	1.5166	18	2.08± .01	2.088	1.4859	1.4888
5	2.18± .01	2.151	1.5151	1.5179	19	2.08± .01	2.103	1.4920	1.4977
6	2.18± .02	2.181	1.5117	1.5149	20	2.09± .01	1.987	1.5066	1.5026
7	2.18± .01	2.186	1.5145	1.5164	21	2.08± .01	2.040	1.4933	1.4975
8	2.06± .01	2.066	1.5007	1.4966	22	2.06± .01	2.087	1.4917	1.4971
9	2.06± .01	2.122	1.4835	1.4877	23	n.d.	2.062	n.d.	n.d.
10	2.06± .01	2.063	1.4874	1.4846	24	2.10± .01	2.087	1.4879	1.4941
11	2.15± .01	2.187	1.5034	1.5071	25	2.08± .01	2.063	1.4898	1.4974
12	2.06± .01	2.073	1.4894	1.4927	26	n.d.	2.085	n.d.	n.d.
13	2.08± .01	2.090	1.4962	1.4994	27	n.d.	2.106	1.488	1.487
14	2.07± .01	2.077	1.4921	1.4944	28	n.d.	1.967	1.460	1.462

Numbers of samples are the same as Table 1 and 2.
No. 1 to No. 25: values measured by author.
No. 23: it was not possible to measure the density and the refraction indices because the sample was received as a powder.
No. 26: data not available.
No. 27: refraction indices by Weibel (1963).
No. 28: refraction indices by Gude and Sheppard (1966).

3) $M/(M+B)$ = (sum of the atomic coefficients of the monovalent exchangeable cations)/(sum of the atomic coefficients of all exchangeable cations). The correlation matrices obtained for a and c, are:

	a	R	$M+B$	$M/(M+B)$
a	1.000	−0.352	0.475	0.274
R		1.000	−0.685	−0.105
$M+B$			1.000	0.755
$M/(M+B)$				1.000

	c	R	$M+B$	$M/(M+B)$
c	1.000	−0.931	0.595	0.111
R		1.000	−0.685	−0.105
$M+B$			1.000	0.755
$M/(M+B)$				1.000

The parameter a shows a major correlation with $M+B$ and a minor one with $M/(M+B)$. The best regression equation (level of probability slightly lower than 99%) is:

$$a = 13.74961 + 0.02130(M+B) \quad F\text{-ratio} = 7.286$$

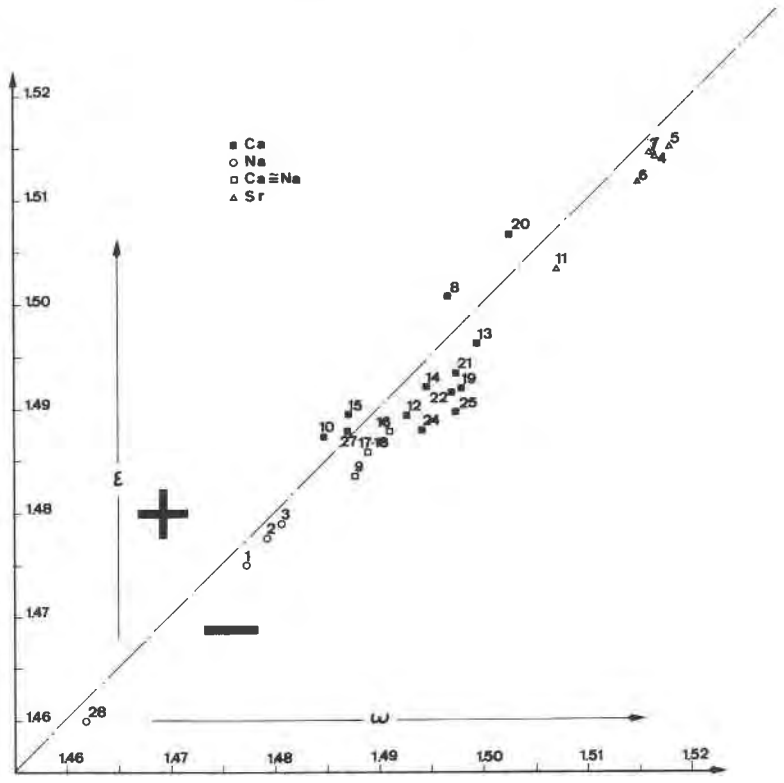

FIG. 5. Variation of refractive indices. Solid square: Ca-chabazites; hollow circle: Na-chabazites; hollow square: intermediate Ca-Na samples; hollow triangle: Ca-chabazites with more than 3% of SrO.

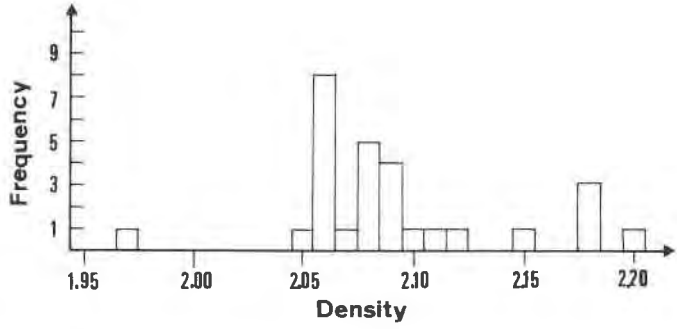

FIG. 6. Frequency distribution of densities.

TABLE 5. CORRELATION MATRICES FOR REFRACTIVE INDICES

	ϵ	R	H_2O	PCS	$M/(M+B)$	Fe_2O_3
ϵ	1.000	−0.629	0.459	0.634	−0.530	0.222
R		1.000	−0.364	−0.935	−0.102	0.062
H_2O			1.000	0.280	−0.471	−0.248
PCS				1.000	0.101	−0.094
$M/(M+B)$					1.000	0.001
Fe_2O_3						1.000
	ω	R	H_2O	PCS	$M/(M+B)$	Fe_2O_3
ω	1.000	−0.662	0.482	0.666	−0.541	0.082
R		1.000	−0.364	−0.935	−0.102	0.062
H_2O			1.000	0.280	−0.471	−0.248
PCS				1.000	0.101	−0.094
$M/(M+B)$					1.000	0.001
Fe_2O_3						1.000

The parameter c shows a very close correlation with R and a minor one with $M+B$. The most significant regression equation (level of probability more than 99%) is:

$$c = 16.98639 - 2.78039(R) \quad F\text{-ratio} = 162.674$$

Through the same program of correlation the regression equations for estimating the above-mentioned chemical variables from measured values of physical parameters was calculated.

The equations for estimating R and $M+B$ from measured values of a and c, respectively, show a very good and acceptable value of standard error of estimation since the standard deviation of R is 0.04874 and that of $M+B$ is 0.67064:

$$9.48768 - 0.30971a - 0.30030c = R \pm 0.0181$$

$$-151.38509 + 8.49099a + 2.42874c = (M+B) \pm 0.4962$$

The equations for estimating PCS and Fe_2O_3 from measured values of ϵ and ω, on the other hand, show standard errors of estimation almost equal to their standard error of deviation and therefore they are not reported. The equation:

$$15.59341 - 10.16743\omega = (M/(M + B)) \pm 0.2124$$

allows only an appropriate estimation of $M/(M+B)$ since the standard deviation of this chemical parameter is 0.24742.

Some Features of the X-ray Diffraction Powder Patterns of Chabazites

Because of the correlation between unit-cell dimensions, Si/(Si+Al+Fe) ratio and exchangeable cation content, X-ray diffraction powder patterns of three samples of different chemical composition were made in order to emphasize the differences in the number, position and intensity of reflections. As cleavage in chabazite is not marked, no precautions were taken to avoid preferred orientation. The three samples chosen for this purpose are Nos. 1, 4 and 13. The X-ray diffraction powder patterns obtained with the Guinier-De Wolff camera are shown in Table 6 together with the X-ray diffraction powder data of sample No. 28 reported by Gude and Sheppard (1966).

If the X-ray diffraction powder pattern of No. 13 is taken as a point of reference, being obtained on a sample of chemical composition corresponding to that of most chabazites, it is observed that the $d(hk\bar{i}l)$ values with large l increase in Nos. 1 and 4 (samples with a low Si/(Si+Al+Fe)ratio) and decrease in No. 28 (sample with a high Si/(Si+Al+Fe) ratio). In sample No. 4, the overlap of $(40\bar{4}1)$ and $(21\bar{3}4)$ reflections in a single line at 2.915 Å is particularly significant. In sample No. 1, moreover, an increase of $d(hk\bar{i}l)$ values with large h is noted. This, as has already been seen, is correlated with the great number of exchangeable cations in the mineral. As for the number and intensity of reflections, few differences are observed between Nos. 1, 4 and 13; this comparison is not available for the data of No. 28, since they were obtained by the diffractometer method.

The position of the reflections of all samples considered in this work, measured with a diffractometer calibrated with quartz, enabled us to plot a diagram (Fig. 7) where the 2θ values of reflections are versus Si/(Si+Al+Fe) ratio. For the sake of greater clarity and precision only the strongest reflections between 20° and 50° were considered. From Figure 7 it appears that the lines representing the $(hk\bar{i}l)$ reflections with small l are vertical, while those representing the $(hk\bar{i}l)$ reflections with large l are more or less inclined according to the l value.

Behavior on Heating

Mumpton (1960) reported that clinoptilolite and heulandite differ because of their behavior on heating. Alietti (1967) stated that the distinctive chemical characteristic of the two minerals is their different content of monovalent and bivalent cations.

In order to find out whether the different content of monovalent and bivalent cations causes a different behavior on heating in chabazite as

TABLE 6. X-RAY DIFFRACTION POWDER DATA OF SAMPLES NOS. 1, 4, 13 AND 28.

	28		13		1		4	
hkīl	*d*(Å)	*I*	*d*(Å)	*I*[a]	*d*(Å)	*I*[a]	*d*(Å)	*I*[a]
10$\bar{1}$1	9.263	70	9.30	s	9.50	s	9.50	s
11$\bar{2}$0	6.846	22	6.94	mw	6.94	w		
10$\bar{2}$2	6.298	8	6.32	vw				
20$\bar{2}$1	5.514	32	5.55	m	5.62	w	5.55	w
0003	4.959	38	5.02	m	5.11	m	5.11	m
20$\bar{2}$2	4.643	4			4.70	vw	4.70	vw
21$\bar{3}$1	4.293	100	4.29	vs	4.36	s	4.33	ms
11$\bar{2}$3	4.020	5						
30$\bar{3}$0	3.957	5	3.97	vw	4.00	vw	3.97	w
21$\bar{3}$2	3.844	20	3.86	m	3.91	m	3.88	mw
10$\bar{1}$4	3.549	47	3.56	ms	3.62	m	3.66	mw
22$\bar{4}$0	3.427	21	3.45	mw	3.46	m	3.44	vw
31$\bar{4}$1	3.217	10	3.22	vw	3.25	vw		
20$\bar{2}$4	3.152	11	3.17	vw	3.21	vw	3.22	vw
30$\bar{3}$3	3.056	2						
31$\bar{4}$2	3.011	1						
40$\bar{4}$1	2.911	62	2.910	vs	2.947	s		
10$\bar{1}$5	2.885	22					2.915	vs
21$\bar{3}$4	2.864	34	2.878	ms	2.910	m		
22$\bar{4}$3	2.820	6	2.820	vw				
40$\bar{4}$2	2.7575	3	2.761	vw	2.795	vw	2.765	vw
32$\bar{5}$1	2.6812	2						
20$\bar{2}$5	2.6619	6	2.669	vw	2.712	vw	2.720	vw
41$\bar{5}$0	2.5909	11	2.587	w	2.612	ms	2.590	ms
32$\bar{5}$2	2.5565	3			2.579	vw		
21$\bar{3}$5	2.4806	12	2.489	m	2.523	ms	2.530	ms
40$\bar{4}$4	2.3224	1			2.447	vw		
41$\bar{5}$3	2.2979	2			2.322	vw		
33$\bar{6}$0	2.2855	2			2.305	vw	2.277	vw
50$\bar{5}$2	2.2629	4						
42$\bar{6}$2	2.1493	1						
40$\bar{4}$5	2.1026	3			2.130	vw		
33$\bar{6}$3	2.0759	6	2.074	w	2.097	w	2.083	w
50$\bar{5}$4	2.0018	2			2.069	w		
6060	1.9794	1						
43$\bar{7}$1	1.9356	2			1.951	vw		
21$\bar{3}$7	1.9201	2						
52$\bar{7}$0	1.9012	5			1.911	vw		
50$\bar{5}$5	1.8563	9	1.896	vw	1.873	vw		
60$\bar{6}$3	1.8381	3	1.857	vw				
41$\bar{5}$6	1.7918	12	1.791	m	1.807	ms	1.811	vw
20$\bar{2}$8	1.7752	2						
61$\bar{7}$2	1.7590	8						
44$\bar{8}$0	1.7149	8	1.710	mw	1.722	m		
33$\bar{6}$6	1.6811	4	1.679	w	1.698	w	1.707	w
0009	1.6537	4	1.656	w	1.674	w		
62$\bar{8}$1	1.6364	6	1.630	vw	1.643	mw	1.630	vw
40$\bar{4}$8	1.5764	2						
60$\bar{6}$6	1.5466	5	1.543	w	1.557	w	1.553	w

Nos. 1, 4 and 13: data obtained by the author with Guinier-De Wolff camera (CuKα radiation)

No. 28: data obtained by Gude and Sheppard (1966) with diffractometer method (Cu*K*α radiation, Ni filter).

[a] vs, very strong; s, strong; ms, medium to strong; m, medium; mw, medium to weak; w, weak; vw, very weak.

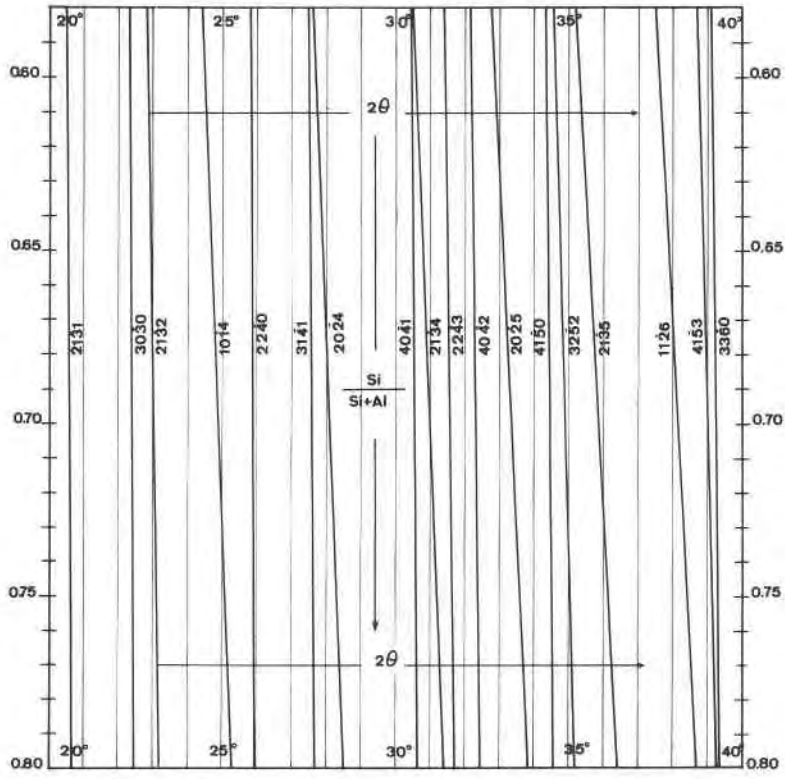

FIG. 7. Variation of 2θ (CuKα radiation, Ni filter) of main powder lines versus Si/(Si+Al+Fe) ratio.

well, X-ray diffraction powder patterns of three previously heated samples were made. These samples, chosen that they represented three chemically different types, were:

No. 1 (Na rich member; Si/(Si+Al+Fe) ratio = 0.620)
No. 4 (Ca, Sr and K rich member; Si/(Si+Al+Fe) ratio = 0.587)
No. 13 (Ca rich member; Si/(Si+Al+Fe) ratio = 0.670)

Each of these samples has been heated for 10 hours at the following temperatures: 300, 400, 500, 550, 600, 650, 750, 800, 850°C. After each heating the sample was cooled at room temperature and then the X-ray diffraction powder pattern was taken with Guinier-De Wolff camera.

The total destruction of the framework of the three samples takes place only above 800°C, but their behavior at lower temperatures is different.

No. 1 (Na rich member): at temperatures as low as 300°C the weakest reflections disappear and the strongest ones weaken. The lines at 2.947 and 2.910 Å are united into a single band. As the temperature is increased to 800°C so the reflections gradually decrease in intensity and finally disappear. At 400°C a line appears at 6.41 Å. It increases in intensity as the temperature rises to 650°C; thereafter it weakens and finally disappears above 800°C. At 500°C a weak line appears at 2.80 Å. At 800°C only these three very weak reflections are observed: 9.50, 6.41, and 3.66 Å. At 850°C no line is noted.

No. 4 (Ca, Sr, K rich member): at 300°C all the weak and some of the middle reflections disappear; the strong ones weaken perceptibly except those at 9.50 and 2.915 Å; a weak line appears at 6.60 Å. As the temperature is increased it is noted that most of the reflections disappear much quicker than in sample No. 1. Only the line at 9.50 Å remains even if very weak to 850°C.

No. 13 (Ca rich member): there is no difference between the X-ray powder patterns of the samples heated at 300 and 400°C and that of the unheated sample. Up to 650°C the disappearance of a few very weak reflections is observed, while the intensity of the others does not weaken. At 700 and 750°C a few more weak lines disappear; at 800°C some rare, very weak reflections remain. At 850°C no lines are observed.

From these results the following conclusions can be drawn: the chabazite rich in Ca shows a remarkable resistance to increased temperature and the crystalline framework does not suffer any change up to 400°C. The destruction of the framework begins only after 750°C and is quickly completed within a short temperature range. The chabazite rich in Ca, Sr and K is almost totally destroyed at temperatures as low as 400°C, only the fundamental motif of the framework remaining. The complete destruction of the framework takes place after 400°C in a progressive, slow manner. The behavior of the chabazite rich in Na falls between that of the two samples previously described. Slight structural changes begin at 400–500°C and the destruction of the framework takes place in a slow and progressive manner from 550–600°C and is complete at 800–850°C.

The DTA analyses of these three samples were also performed. The DTA curves, marked with the numbers 1, 4, 13 corresponding to the above mentioned samples, are shown in Figure 8. These curves have the following features:

No. 1: a double endothermic peak at 150 and 210°C; a small and very broad exothermic peak at 850°C.

No. 4: a double endothermic peak at 100 and 225°C; a small and very broad exothermic peak at 820°C.

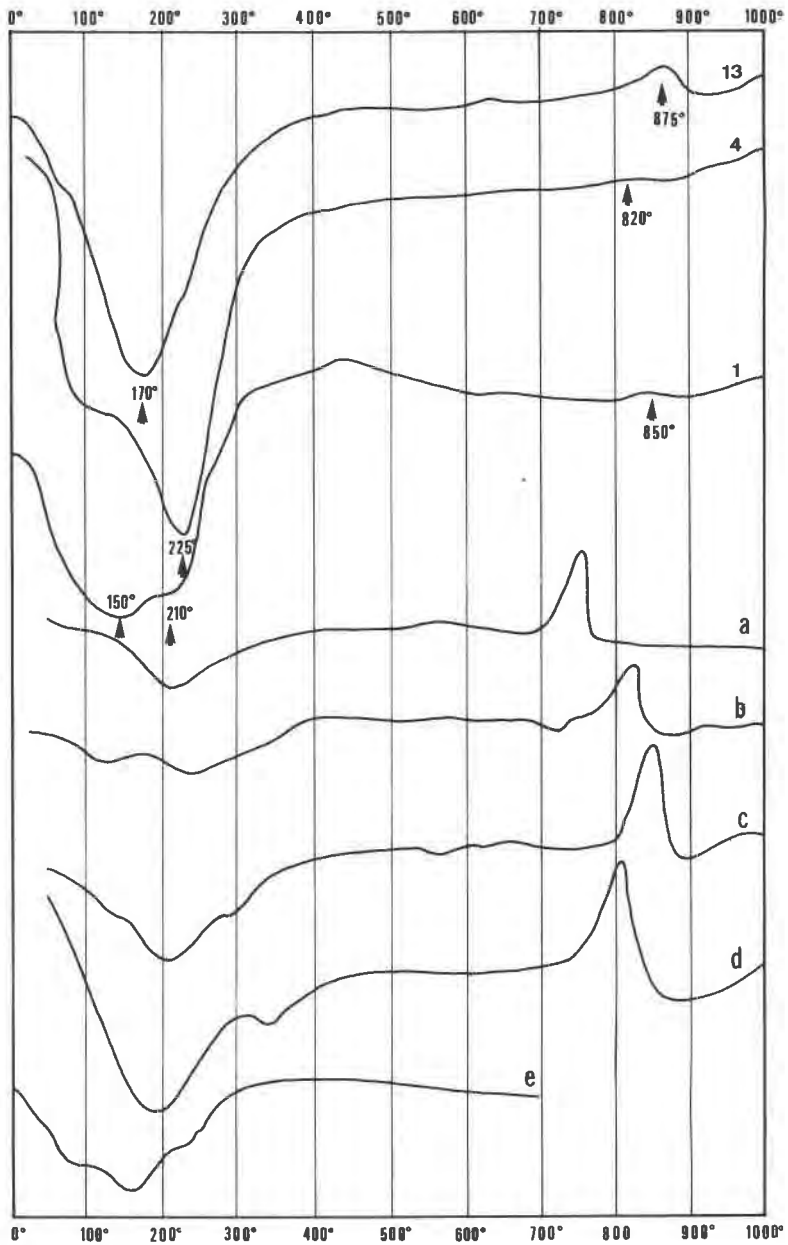

FIG. 8. DTA curves of chabazites. Nos. 1, 4 and 13 as in Table 1; a, b, c, by Pécsi-Donáth (1965); d, bv Kostov (1962); e, by Koizumi (1953).

No. 13: an almost symmetric endothermic peak at 170°C and a very small break at 225°C; a rather sharp exothermic peak at 875°C.

From the comparison of the three DTA curves can be seen that:

a) Water loss always takes place in the same temperature range;
b) The water loss of No. 13 (Ca rich member) occurs in a regular and uniform manner; that of No. 1 (Na rich member) occurs in a very irregular manner and its DTA curve would seem to indicate that dehydration takes place at two different temperatures (150°C and 210°C); that of No. 4 (Ca, Sr, K rich member) also seems to occur at two different temperatures (100 and 225°C), but, unlike No. 1, with magnitude of peaks inverted;
c) The exothermic peak is sharp and very clear only for No. 13, while it is very small for Nos. 1 and 4.

The DTA curves of chabazites are reported in literature by Kostov (1962), Pécsi-Donáth (1965), Majer (1953), and Koizumi (1953). These curves (Figure 8) are marked with the letters a, b, c, d, e, corresponding to the following samples:

a) chabazite of Dunabogdány (Hungary). Sample with 9.00 CaO, 0.97 Na_2O, and 0.33 percent K_2O; Si/(Si+Al+Fe) ratio=0.69 (Pécsi-Donáth, 1965);
b) chabazite of Strzegom (Poland). Sample with 8.43 CaO, 0.25 Na_2O, and 1.67 percent K_2O; Si/(Si+Al+Fe) ratio=0.68 (Pécsi-Donáth, 1965);
c) chabazite of Szob (Hungary). Sample with 10.59 CaO, 0.54 Na_2O, and 0.23 percent K_2O; Si/(Si+Al+Fe) ratio=0.69 (Pécsi-Donáth, 1965);
d) chabazite of Lipata (Bulgaria). Sample with 7.51 CaO, 1.09 Na_2O, and 2.80 percent K_2O; Si/(Si+Al+Fe) ratio=0.70 (Kostov, 1962);
e) chabazite of Mitaki Sendai (Japan). Sample with 10.09 CaO, and 1.34 percent Na_2O; Si/(Si+Al+Fe) ratio=0.66 (Koizumi, 1953).

The feature of these curves only partially confirms what can be observed from curves Nos. 1, 4, 13. In fact, while the exothermic peak is sharp and very clear only in the samples with a low content of monovalent cations and with a Si/(Si+Al+Fe) ratio greater than 0.65, the feature of the endothermic peak is variable and it does not seem to follow steady rules.

Conclusions

The results of this research show that the chemical composition of chabazite varies considerably. As for the content of exchangeable cations, Ca-chabazite are more frequent than Na-chabazites. The existence of

samples of intermediate composition excludes a compositional gap between the two end members, as supposed by Mason (1962). Though a K rich member do not exists, some samples show a remarkable content of this element, and in these samples a high content of Sr is always observed.

The Si/(Si+Al+Fe) ratio shows considerable variations. At this point it is opportune to remark that, while in clinoptilolites the high content of Si corresponds to that of monovalent exchangeable cations and vice versa in heulandites, such correspondence is not observed in chabazites (except No. 28). This leads one to suppose, in agreement with Mason (1962), that replacements of type $Na_2(K_2)\rightleftarrows Ca$ are much more frequent than those of type $Na(K)Si\rightleftarrows CaAl$.

About the unit-cell dimensions, as a general rule it can be said that c increases with the Al content and, moreover, that a increases with the number of exchangeable cations, especially when Na is predominant. Barrer and Sammon (1955) report a and c values for Na-exchanged chabazites which are higher than those for Ag, Ca, Ba-exchanged forms. Smith (1962), however, states that the value of a is lower in Na-chabazite (hydrated) than in Ca-chabazite (hydrated), while the c value is higher in the first form. From measured values of a and c, it is possible, by means of an equation, to find out the Si/(Si+Al+Fe) ratio and the sum of exchangeable cations.

The refractive indices increase with the Al content, especially when Sr and Ba are present among the exchangeable cations. The Na content, on the other hand, causes a considerable lowering of the value of ϵ and ω even in those samples with a low Si/(Si+Al+Fe) ratio. This is probably partly due to the fact that the Na cation causes a less hydrated condition.

The densities depend both on the Si/(Si+Al+Fe) ratio and on the type of exchangeable cation.

The X-ray diffraction powder patterns of three samples with different chemical composition have differences in the position of the reflections.

The behavior on heating of these three samples showed that the destruction of the framework takes place in a somewhat different way. The DTA curves are also different. In a further study the different types of chabazites could be classified in accordance with their behavior when heated.

Lastly, it must be stressed that silica-rich chabazite (No. 28) is found in rhyolitic volcanic glass in a sedimentary environment, while chabazites with a low Si content are found in cavities of very basic igneous rocks (basalts, nephelinite-tephrites, leucitites).

ACKNOWLEDGMENTS

Thanks are due to: G. Gottardi for some useful suggestions and for his critical review of the manuscript; P. Černý for sending the five samples with their chemical analyses; C.

Sandi (IBM, Pisa) for the kind permission to use the BMD O2R stepwise multiple regression program; G. C. Bocchi (University of Bologna) for the DTA curves; A. G. Loschi Ghittoni (University of Modena) for her help in performing part of the chemical analyses.

For some samples studied in this research thanks are due to: G. Scaini (Milano); M. Franzini (University of Pisa); V. De Michele (Museo Civico di Storia Naturale of Milano); B. Mason and J. White (U. S. National Museum, Washington); F. L. Sutherland (Tasmanian Museum of Hobart); R. J. W. MacLaughlin (University of Melbourne); L. Ogniben and M. Riuscetti (University fo Catania).

This work was made possible through financial support of Consiglio Nazionale delle Ricerche, Roma.

References

Alietti, A. (1967) Heulanditi e clinoptiloliti. *Mineral. Petrogr. Acta*, **13**, 119–138.

Barrer, R. M. (1958) Crystalline ion-exchangers. *Proc. Chem. Soc.* **1958**, 99.

——— and D. C. Sammon (1955) Exchange equilibria in crystals of chabazite. *J. Chem. Soc.* **1955**, 2838–2849.

Becke, F. (1880) Uber die Zwillingsbildung und die optischen Eigenschaften des Chabasit. *Tschermaks Mineral. Petrologr. Mitt.* **2**, 391–419.

Berman, H. (1939) A torsion microbalance for the determination of specific gravities of minerals. *Amer. Mineral.* **24**, 434–440.

Breck, D. W., W. G. Eversole, R. M. Milton, T. B. Reed, and T. L. Thomas (1956) Crystalline zeolites. I. The properties of a new synthetic zeolite, type A. *J. Amer. Chem. Soc.* **78**, 5963–5971.

Caglioti, V. (1927) Ricerche sulla composizione chimica della herschelite di Acicastello. *Rend. Accad. Sci. Fis. Mat. Napoli, ser. 3*, **33**, 156–163.

Capola, A. (1948) L'herschelite di Palagonia (Catania). *Notiz. Mineral. Sicil. Calabrese.* **2**, 63–69.

Černý, P., and P. Povondra (1965) New occurrence of strontian chabazite. *Acta Univ. Carol. Geol.* **2**, 163–174.

Charlot, G. (1961) *Les méthodes de la chimie analytique. Analyse quantitative minérale.* Masson et C. ie, Paris.

Coombs, D. S., A. J. Ellis, W. S. Fyfe, and A. M. Taylor (1959) The zeolites facies, with comments on the interpretation of hydrothermal syntheses. *Geochim. Cosmochim. Acta.* **17**, 53-107.

De Michele, V., and G. Scaini (1968) Tre nuovi giacimenti zeolitici nelle Alpi piemontesi. *Natura*, **59**, 145–148.

Dent, L. S., and J. V. Smith (1958) Crystal structure of chabazite, a molecular sieve. *Nature* **181**, 1794–1796.

Di Franco, S. (1942) *Mineralogia Etnea.* Zuccarello & Izzi, Catania.

Doelter, C. (1921) *Handbuch der Mineralchemie. Band II, 3 Teil.* Steinkopff, Dresden und Leipzig.

Dunham, K. C. (1933) Crystal cavities in lavas from the Hawaiian Islands. *Amer. Mineral.* **18**, 369–385.

Foster, M. D. (1965) Studies of the zeolites. Compositional relations among thomsonites, gonnardites, and natrolites. *U.S. Geol. Surv. Prof. Pap.* **504-E**.

Gude, A. J., and R. A. Sheppard (1966) Silica-rich chabazite from the Barstow formation, San Bernardino County, Southern California. *Amer. Mineral.* **51**, 909–915.

Hewett, D. F., E. V. Shannon, and F. A. Gonyer (1928) Zeolites from Ritter hot spring, Grant County Oregon. *Proc. U.S. Nat. Mus.*, **73**, (art. 16), pp. 18.

Hodge-Smith, T. (1929) The occurrence of zeolites at Kyogle, New South Wales. *Rec. Aust. Mus.* **17**, 279–290.

IRRERA, G. (1949) Herschelite in basalto palagonitico da un sondaggio a Ficarazzi (Catania) *Notiz. Mineral. Sicil. Calabrese.*, **3**, 40–47.

KAPPEN, H., AND B. FISCHER (1928) Ueber den Ionenaustausch der zeolithischen Silikate bei Beteiligung hydrolytisch gespaltener Salze. 2. Mitteilung. Versuche mit natürlichen Silikaten. *Z. Pflanzener Düngung. Bodenk. A*, **12**, 2–37.

KATO, T. (1959) Heulandite and chabazite from Hashikaké-zawa, Chichibu mine, Saitana Prefecture. *Mineral. J.* [Tokyo], **4**, 299–306.

KOIZUMI, M. (1953) The differential thermal analysis curves and dehydration curves of zeolites. *Mineral. J.* [Tokyo], **1**, 36–47.

KOSTOV, I. (1962) The zeolites in Bulgaria; analcime, chabazite, harmotomo. *God. Sofii. Univ. Biol. Geol. Geogr. Fak. Kn. 2-Geol.*, **55**, 159–174.

MAJER, V. (1953) Chabazite and Stilbite from Bor (Yugoslavia). *Jugoslav. Akad. Znan. Umjet.*, 175–192.

MASON, B. (1955) Notes on some New Zealand minerals. *N. Z. J. Sci. Tech., B*, **36**, 557–560.

——— (1962) Herschelite—a valid species? *Amer. Mineral.*, **47**, 985–987.

———, AND S. S. GREENBERG (1954) Zeolites and associated minerals from southern Brazil. *Ark. Mineral. Geol.* **1**, 519–526.

MAVRUDČIEV, B., L. FILIZOVA, G. N. KIROV, AND I. KOSTOV (1965) Magmatism and zeolitization at the Pb-Zn deposit near Madžarovo. *Acad. Bulg. Sci. Trav. Geol. Bulg. Ser. Geochem. Mineral. Petrogr.* **5**, 273–297.

MORGANTE, S. (1945) Zeoliti della zona di Dessiè e Diredaua in A. O. *Atti Ist. Veneto Sci. Lett. Arti*, **104**, 405–425.

MORSE, H. N., AND H. S. BAYLEY (1884) Ueber den Haydenit. *J. Amer. Chem. Soc.*, **6**, 24. [*Z. Kristallogr.*, **10**, 318–319. (1888)].

MUMPTON, F. A. (1960) Clinoptilolite redefined. *Amer. Mineral.*, **45**, 351–369.

NIGGLI, P., J. KOENIGSBERGER, AND R. L. PARKER (1940) *Die mineralien der Schweizeralpen.* **2**, Wepf-Verlag, Basel.

NOWACKI, W., H. KOYAMA, AND M. H. MLADECK (1958a) Über die Kristall structur des Zeolithes Chabasit. *Experientia*, **14**, 396.

———, M. AELLEN, AND H. KOYAMA (1958b) Einige Röntgendaten über Chabasit Gmelinit und Lévyn. *Schweiz. Mineral. Petrogr. Mitt.* **38**, 53–60.

PASSAGLIA, E. (1969) Le zeoliti di Albero Bassi (Vicenza). *Period. Mineral.* **38**, 237–243.

PÉCSI-DONÁTH, É. (1965) On the individual properties of some hungarian zeolites. *Acta Acad. Geol. Sci. Hung.* **9**, 235–259.

RABINOWITCH, E., AND W. C. WOOD (1936) Ionic exchange and sorption of gases by chabasite. *Trans. Faraday Soc.*, **32**, 947–956.

REICHERT, R., AND J. ERDELYI (1935) Über die Minerale des Csódi-Berges bei Dunabogdány (Ungarn). *Tschermak's Mineral. Petrogr. Mitt.* **46**, 237–255.

RIMATORI, C. (1900) Sulle cabasiti di Sardegna e della granulite di Striegau nella Slesia. *Rend. Reale Accad. Lincei*, **9**, (II), 146–151.

SCAINI, G., AND A. GIORGETTA (1967) Alcuni minerali di Courmayeur (Aosta). *Rend. Soc. Mineral. Ital.*, **23**, 399–404.

SHKABARA, M. N. (1941) Zeolites of the Mama-Vitim mica-bearing region. *Dokl. Akad. Nauk SSSR*, **32**, 420–423.

SMITH, G. F. HERBERT (1961) Chabazite and associated minerals from County Antrim. *Mineral. Mag.* **17**, 274–304.

SMITH, J. V. (1962) Crystal structures with a Chabazite Framework. I. Dehydrated Ca-Chabazite. *Acta Crystallogr.* **15**, 835–845.

———, F. RINALDI, AND L. S. DENT GLASSER (1963) Crystal structures with a Chabazite

Framework. II. Hydrated Ca-Chabazite at Room Temperature. *Acta Crystallogr.* **16,** 45–53.

———, R. C. KNOWLES, AND F. RINALDI (1964) Crystal structures with a chabazite framework. III. Hydrated Ca-chabazite at +20° and −150°C. *Acta Crystallogr.* **17,** 374–384.

STOKLOSSA, G. (1918) Über die Natur des Wassers in den Zeolithen. *Neues Jahrb. Mineral. Geol. Paleontol.* **42,** 1–64.

TISELIUS, A., AND S. BROHULT (1934) Sorption von Wasserdampf an Chabasit bei verschiedenen Temperaturen. *Z. Physik. Chem. A.*, **168,** 248–256.

TOMKEIEFF, S. I. (1934) Differentation in basalt lava, Island Magee, Co. Antrim. *Geol. Mag.* **71,** 501–512.

WALKER, T. L., AND A. L. PARSONS (1922) The zeolites of Nova Scotia. *Contrib. Can. Mineral.* **14,** 13–73.

WEIBEL, M. (1963) Chabasit vom Chrüzlistock (Tavetsch). *Schweiz. Mineral. Petrogr. Mitt.* **43,** 361–366.

WYART, J. (1933) Recherches sur les zéolites. *Bull. Soc. Fr. Mineral. Cristallogr.* **56,** 81–187.

ZAMBONINI, F. (1902) Kurzer Beitrag zur chemischen Kenntniss einiger Zeolithen der Umgegend Roms. *Neues Jahrb. Mineral. Geol. Paleontol.* **2,** 63–69.

Manuscript received, December 29, 1969; accepted for publication, March 31, 1970.